JOURNAL OF MATERIALS SCIENCE 32 (1997) 1963–1967

Sintering of elemental carbonyl iron and carbonyl nickel powder mixtures

TIEN-YIN CHAN
Mechanical Engineering Department, Far-East College, Tainan, Taiwan
SHUN-TIAN LIN
Mechanical Engineering Department, National Taiwan Institute of Technology, Taipei, Taiwan

Iron-nickel alloys with compositions ranging from pure iron to pure nickel at increments of 10 wt% have been prepared by mixing fine elemental carbonyl iron and nickel powders, and sintering at temperatures between 1200–1350 °C. The addition of nickel to iron promoted densification and avoided abnormal grain growth at low concentrations. However the densification was retarded when the iron and nickel had approximately equivalent concentrations. As the concentration of nickel increased, the room temperature structures of the alloys gradually changed from α-Fe into γ-(Fe, Ni), with Fe–30 wt% Ni and Fe–40 wt%, Ni containing both phases. The relative abundance of each phase was determined by the degree of compositional homogeneity achieved in sintering.

1. Introduction

Nickel is an important alloying element for iron, since it affects its phase transformation kinetics, chemical inertness, and toughness [1–3]. The applications of Fe–Ni based alloys are very diverse which is a function of the wide range of compositions for the alloys, ranging between 2 wt–80 wt% Ni, that are available for use. Carbon steels are usually alloyed with between 2–8 wt% nickel to improve their mechanical properties [1, 2, 4]. On the other hand, iron alloyed with high nickel contents are used for functional applications. For example, alloys with the duplex α and γ structures, such as Fe–36 wt% Ni (Invar) and Fe–42 wt% Ni (Super Invar), are used as controlled expansion materials [5]. In addition, iron–nickel alloys having 45–80 wt% nickel are usually used as high permeability soft magnetic materials [6].

Metal injection molding (MIM) is a process route capable of mass producing high performance components with complex geometries and it is extensively used for iron–nickel based alloys [7]. Unlike conventional powder metallurgy techniques where mixtures of coarse powders are typically used, MIM usually employs fine powders so that improved properties can be attained. The powders used in MIM can be either pre-alloyed powders or mixed elemental powders. For iron or nickel based alloys, utilization of the mixed elemental powders is a cost-effective approach because standard grades of carbonyl iron and carbonyl nickel powders are widely available. Nevertheless, the degree of compositional homogeneity of the sintered alloys using mixed elemental powders can still be lower than those of the equivalent alloys processed with pre-alloyed powders.

The degree of compositional homogeneity is important for the functional applications of iron–nickel alloys because the transformation temperature between the α and γ phases is determined by the alloy composition [1, 3]. Nickel lowers the α–γ phase transformation temperature and retards the transformation kinetics of Fe–Ni alloys during cooling. Therefore, the relative degree of component distribution homogeneity of Fe and Ni elements subsequent to sintering determines the relative abundance of the α and γ phases, and, therefore, the functional properties such as magnetic inductance and thermal expansion of the alloys. Additionally, sintering elemental carbonyl Fe–Ni powder mixtures in the α phase domain can ideally yield alloys with high densities and refined microstructures [8, 9]. Thus, the transformation of the α phase into the γ phase accompanying the interdiffusion between iron and nickel during the sintering cycle can retard the densification of the Fe–Ni alloys.

This study is aimed at investigating the sintering behaviour of various iron–nickel powder mixtures using elemental carbonyl iron and nickel powders. The diffusional homogenization of the elemental powders, and, therefore, the phase evolution as a variation of sintering temperature is investigated. The sintering behaviour, phase evolution, and properties are examined and correlated.

2. Experimental procedure

The powders used in this study were carbonyl iron powder (OM grade, Basf, Germany) and carbonyl nickel powder (INCO 123 grade, Novamet, USA). The characteristics of the powders are listed in Table I.

0022–2461

TABLE I The characteristics of the carbonyl iron and nickel powders

		Iron		Nickel
Vendor		BASF		INCO
Grade		OM		123
Mean particle size (μm)		4.5		9.8
Apparent density ($g\,cm^{-3}$)		2.7		2.2
Tap density ($g\,cm^{-3}$)		4.3		3.6
Major impurities (wt%)	C	0.89	C	0.10
	N	0.90	O	0.15
	O	0.30	Fe	0.01

Eleven iron–nickel alloys with compositions ranging from pure iron to pure nickel at increments of 10 wt% were prepared by ball-milling the powder mixtures in heptane for 24 h. Paraffin wax, which served as die lubricant and binder, was added to the extent of 2 wt% of the powder to be ball milled. Subsequent to ball-milling, the powder mixtures were dried at 80 °C for 6 h and then graded with an 80 mesh sieve.

The graded powder granules were uniaxially pressed with a pressure of 100 MPa into cylindrical specimens 13 mm in diameter and 15 mm in length. These specimens were sintered in a tube furnace heated at a rate of 10 K min^{-1} to temperatures between 1200–1350 °C, and soaked for 1 h in a dry hydrogen atmosphere. Dilatometric tests were also conducted on the specimens using a heating ramp of 10 K min^{-1}. The density was measured using the water immersion method, and the residual carbon content was measured by the combustion method (Leco CS-244). The hardnesses of the alloys were measured using both the Rockwell hardness (B scale) test and also the Vickers micro-hardness test. Phase analysis of the bulk sintered specimens was performed using X-ray diffraction (XRD, Rigaku DMAX-B) with Cu K_α radiation at an accelerating voltage of 40 keV.

3. Results and discussion

After the sintering at temperatures between 1200–1350 °C, the residual carbon contents of the iron–nickel alloys varied in the range of 140–175 ppm, without a meaningful statistical trend. Even though the initial carbon contents of the eleven powder mixtures were between 0.1 wt% (100 wt% nickel) and 0.9 wt% (100 wt% iron), the residual carbon contents of the sintered alloys were reduced by the hydrogen atmosphere to levels that are approximately equivalent in scale to those usually achieved in cast alloys. In fact, the decarburization of the carbonyl iron powder by the hydrogen atmosphere was almost completed at temperatures lower than 700 °C [10]. Therefore, any possible effects due to residual carbon content on the phase structure and physical properties are ignored in the following discussion.

Fig. 1 shows the XRD patterns of the iron–nickel alloys sintered at 1350 °C. With Fe–30 wt% Ni as the transitional composition, the alloys in the iron rich side were composed of α-Fe while those in the nickel rich side were composed of γ-(Fe, Ni). Even after sintering at a temperature of 1350 °C, the alloy with a composition of Fe–30 wt% Ni still possessed a duplex structure that was composed of both α-Fe and γ-(Fe, Ni) phases. This observation indicated that compositional homogenization was not fully achieved. In fact, due to the low interdiffusion coefficients of Fe and Ni [11], very obvious isolated grains or grain clusters rich in nickel could still be found in the microstructures of iron–nickel alloys sintered at 1250 °C [12].

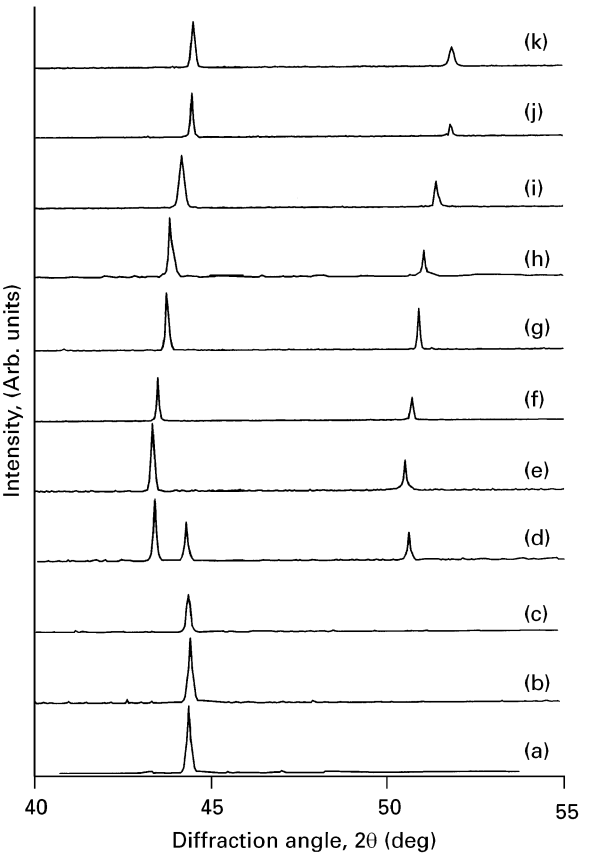

Figure 1 X-ray diffraction patterns of Fe–Ni alloys sintered at 1350 °C. Key: (a) 100% Fe, (b) 90% Fe–10% Ni (c) 80% Fe–20% Ni, (d) 70% Fe–30% Ni (e) 60% Fe–40% Ni, (f) 50% Fe–50% Ni, (g) 40% Fe–60% Ni, (h) 30% Fe–70% Ni, (i) 20% Fe–80% Ni (j)10% Fe–90% Ni and (k) 100% Ni.

The lattice constant of the γ-(Fe, Ni) phase varied with the alloy composition, which can be seen from the slight shifting of the diffraction angle of the {111} and {002} planes in the XRD patterns. The variation of the lattice constant of γ-(Fe, Ni) with the alloy composition is illustrated in Fig. 2, showing positive deviation from Vegard's law. Such a trend indicated that dilation of the lattice occurred with the mutual alloying of iron and nickel. The maximum degree of deviation from Vegard's law, which occurred at Fe-40 wt% Ni, was more than 0.004 nm, or more than 1% of the lattice constant. Such an observation suggests the possible existence of a defected solid solution for alloys with compositions in the neighbourhood of Fe–40 wt% Ni [13].

Fig. 3 shows the variation of hardness with alloy composition. The alloys with the intermediate compositions were harder than the pure elements, as a

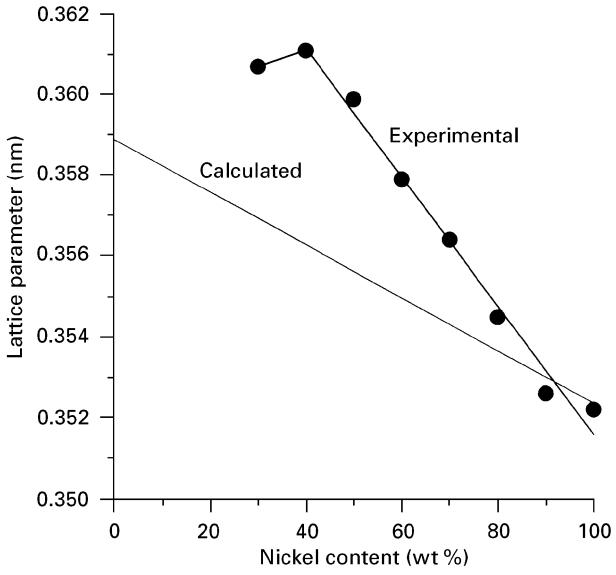

Figure 2 Variation in the lattice constant of γ-(Fe, Ni) with alloy composition. The alloys were sintered at 1350 °C. For comparison purposes the lattice parameter calculated from Vegard's Law is also shown.

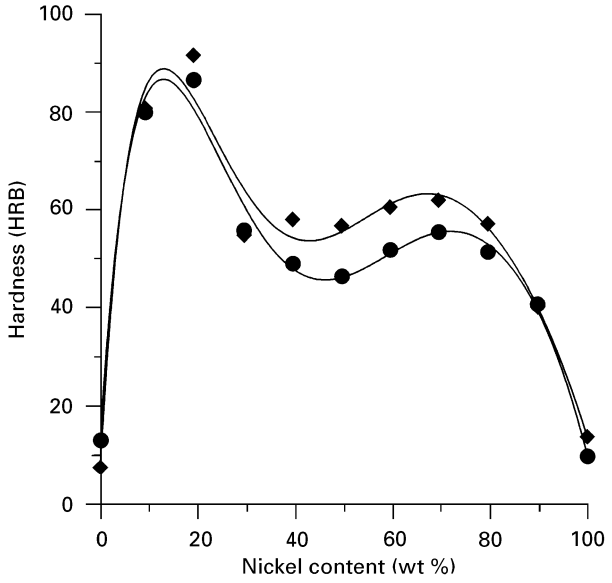

Figure 3 Variation of hardness with alloy composition. The alloys were sintered at (●) 1200 and (◆) 1350 °C for 1 h.

result of solid solution hardening. The solution hardening effect was most significant for the α-Fe phase (Ni < 20 wt%). Indeed, with a nickel concentration in the range between 0–8 wt%, the hardness of the Fe–Ni alloys increased dramatically with the nickel concentration and was less sensitive to porosity [1, 4]. Figs. 4 (a and b) and 5 (a and b) respectively show the microstructures of Fe–30 wt% Ni and Fe–40 wt% Ni sintered at 1300 and 1350 °C. In Fig. 4(b), the heavily etched dark regions had a mean microhardness of 205 Hv̂ while the lightly etched bright regions had a mean microhardness of 118 Hv̂. Apparently, the harder phase was α-Fe and the softer phase was γ-(Fe, Ni). By increasing the sintering temperature from 1300 to 1350 °C, the α-Fe phase in the duplex structure could be eliminated for Fe–40 wt% Ni, but could

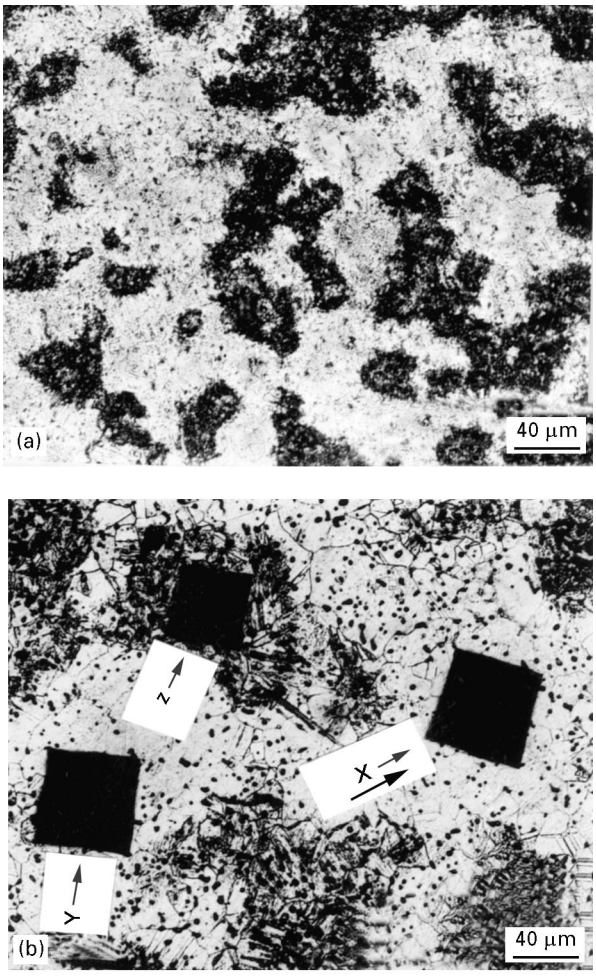

Figure 4 Microstructures of Fe–30 wt%. Ni sintered at (a) 1300 and (b) 1350 °C.

only be reduced to a lower fraction for Fe–30 wt% Ni. This observation indicated that the relative abundance of α-Fe and γ-(Fe, Ni) was determined by the compositional homogeneity achieved in processing, in addition to alloy composition. Thus, process factors such as powder blending variables and the thermal profile during sintering can alter the phase transformation kinetics of Fe–Ni alloys prepared using elemental powders. In turn, the thermal expansion coefficient and magnetic properties of the alloys can also be affected.

Fig. 6 shows the dilatometric curves for Fe, Fe–30 wt% Ni, Fe–50 wt% Ni, and Ni. The carbonyl iron powder mainly densified in the α phase domain and reached the final stage sintering at a temperature above the phase transformation temperature [14]. Thus, high sintered densities with refined microstructures could be achieved by sintering the iron based alloys in the α phase domain [8, 9]. On the other hand, the dilatometric curve of the carbonyl nickel powder exhibited thermally activated densification behaviour so that a high density can only be attained at high sintering temperatures. There was no obvious transitional point, to show an abrupt change of sintering rate caused by phase transformation, in the dilatometric curves of Fe–30 wt% Ni and Fe–50 wt% Ni.

Since nickel reduces the phase transformation temperature of iron alloys, the α-Fe phase transformed

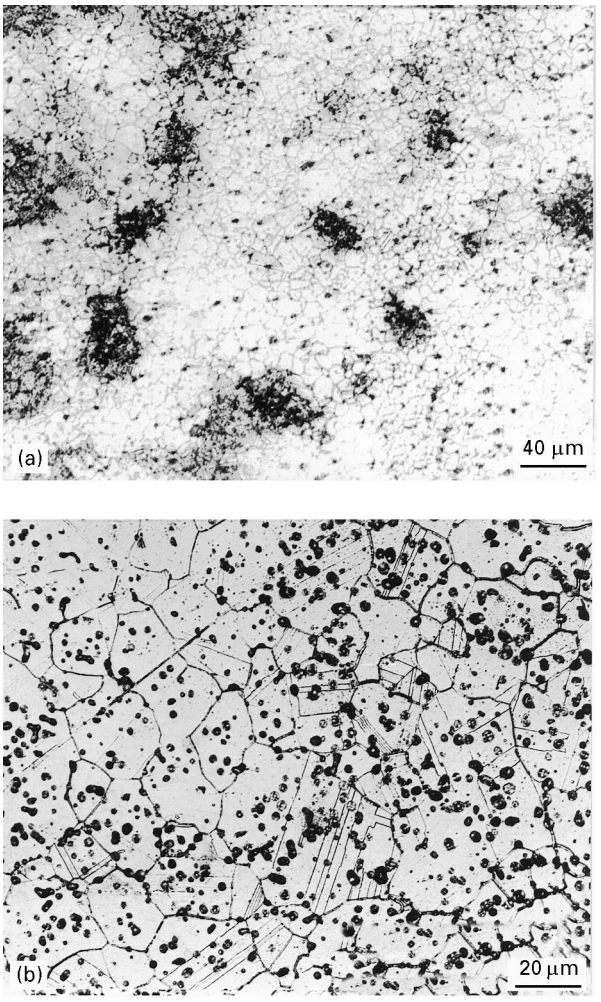

Figure 5 Microstructures of Fe–40 wt% Ni sintered at (a) 1300 and (b) 1350 °C.

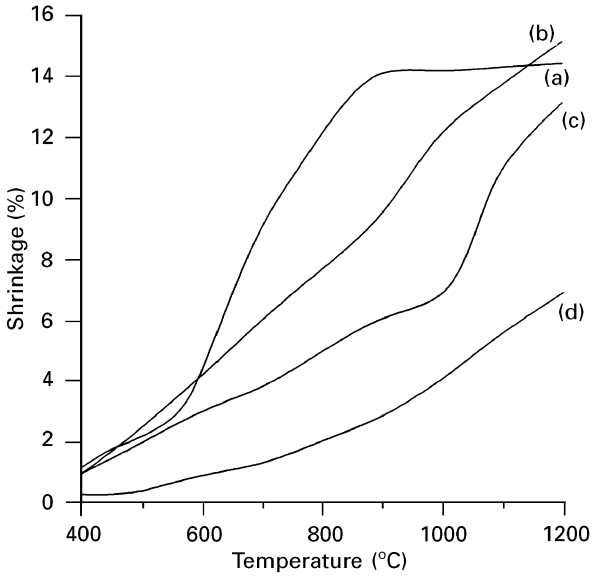

Figure 6 Dilatometric curves of (a) Fe, (b) Fe–30 wt% Ni, (c) Fe–50 wt% Ni, and (d) Ni. The tests were conducted at a ramp of 10 K per min in a hydrogen atmosphere.

into the γ-(Fe, Ni) phase at temperatures lower than the phase transformation temperature of pure iron (918 °C) when interdiffusion between iron and nickel powders occurred. The interdiffusion coefficient near

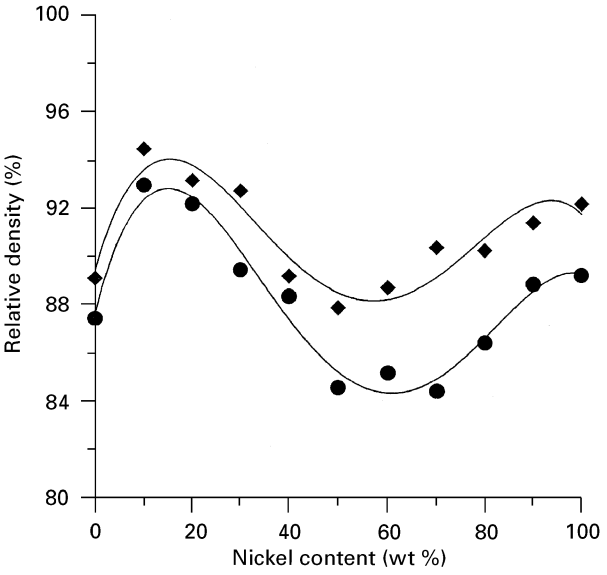

Figure 7 Variation of the sintered density as a function of the alloy composition. The alloys were sintered at (●) 1200 and (◆) 1350 °C for 1 h.

the interdiffusion zone, and, therefore, the sintering rate were thus reduced. In fact, the shrinkage observed in the dilatometric curves for Fe–30 wt% Ni and Fe–50 wt% Ni was the result of the combination of densification shrinkage and phase transformation shrinkage. In comparison, previously published data [4, 15] suggested that the increase in the interdiffusion coefficient with the alloying of nickel to iron powder is beneficial to densification. Such a suggestion was not observed in the dilatometric curves, but could be valid when the sintering temperature was higher than the phase transformation temperature of pure iron.

For elemental powder mixtures, differential stresses possibly existed near the phase interfaces during sintering that tended to retard the densification [1]. In fact, the microscopically inhomogeneous distribution of nickel powder in the iron matrix or *vice versa* led to the emergence of a differential sintered shrinkage stress between the iron and nickel phases. A differential stress also developed near the interdiffusion zone of the iron and nickel where the phase transformation of α-Fe into γ-(Fe, Ni) caused differential volume shrinkage.

The variations in the sintered density and average grain size with alloy composition are shown in Figs. 7 and 8. Even though the carbonyl iron powder had a high sintering potential in the α phase domain, its sintered density was relatively low, due to the abnormal grain growth in the final stage of sintering [8]. The addition of nickel to iron was beneficial to densification only at low nickel concentrations. The abnormal grain growth of carbonyl iron could be effectively controlled by the dissolution of nickel into the iron matrix. Consequently, the attainment of the highest sintered density near the composition of Fe–10 wt% Ni was caused by the counter effects of the existence of differential stresses in the intermediate stage of sintering and also the suppressed abnormal grain growth in the final stage of sintering.

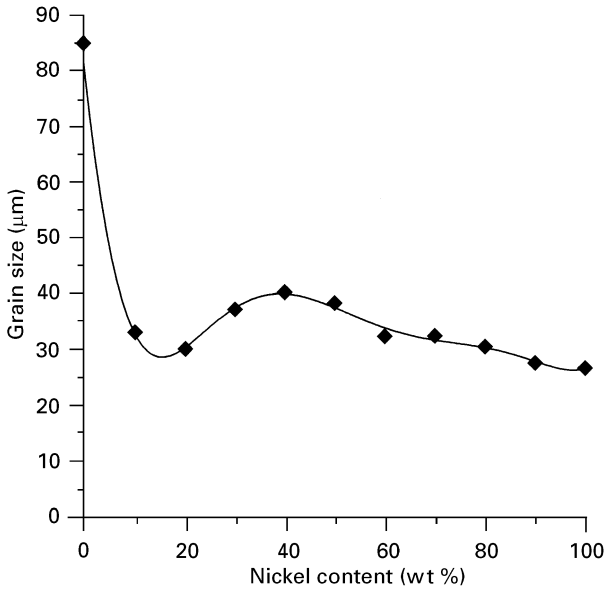

Figure 8. Variation in the average grain size as a function of the alloy composition. The alloys were sintered at 1350°C for 1 h.

The impediment of densification caused by the existence of differential stresses was most pronounced when iron was alloyed with about 60 wt% nickel. The lowest sintered density was attained at this composition, although the interdiffusion coefficients of iron and nickel exhibit a maximum value in the neighbourhood of Fe–60 wt% Ni at temperatures ranging between 1130–1356 °C [11]. Such a trend is analogous to that observed when cobalt-nickel alloys with compositions ranging from pure cobalt to pure nickel were sintered using elemental powder mixtures [16]. The interdiffusion of cobalt and nickel was greatest but the sintered density was the lowest at the composition of Co–50 wt% Ni.

4. Conclusion

Mixtures of elemental carbonyl iron and nickel powders, which are ideal for metal injection molding due to reasons of process economy, suffer two possible problems when iron is alloyed with between 30–80 wt% nickel. The first problem lies in the control of the relative abundances of α-Fe and γ-(Fe, Ni) in the duplex microstructure when the alloys are meant to be used as controlled expansion materials. The relative abundance of the γ-(Fe, Ni) at room temperature depends on (i) the degree of compositional homogeneity achieved in processing and also (ii) the alloy composition. The second problem is due to the observed low sintered density for alloys with 50–80 wt% nickel that limits their use as high permeability soft magnetic materials. Differential stresses evolve as a result of (i) differential shrinkage between the iron and nickel powder clusters during sintering and (ii) transformation of α-Fe into γ-(Fe, Ni) in the interdiffusion zone during sintering. The development of differential stresses in the powder compact impedes densification in the intermediate stage of sintering.

References

1. H. ZHANG and R. M. GERMAN, *Int. J. Powder Metall.* **27** (1991) 249.
2. V. TRACEY, *Metal Powder Report* **28** (1993) 28.
3. W. HUME-ROTHERY, in "The structures of alloys of iron, an elementary introduction" (Pergamon Press, NY, 1966) p. 120.
4. K. S. HWANG and M. Y. HSIAO, in "Powder Injection Molding Symposium-1992", edited by P. H. Booker, J. Gaspervich and R. M. German (Metal Powder Industries Federation, Princeton, NJ, 1992) p. 53.
5. D. WENSCHHOF, in "Metals handbook", Vol. 3, 9th Edn, (American Society for Metals, Metals Park, OH, 1980) p. 792.
6. G. Y. CHIN, L. L. HARNER, M. F. LITTMANN, and J. W. SHILLING, *ibid.* p. 597.
7. R. M. GERMAN, in "Powder Injection Molding", (Metal Powder Industries Federation, Princeton, NJ, 1990) p. 1.
8. B. K. LOGRASSO, A. BOSE, B. J. CARPENTER, C. I. CHUNG, K. F. HENS, D. LEE, S. T. LIN, R. M. GERMAN, R. M. MESSELER, P. F. MURLEY, B. O. RHEE, C. M. SIERRA and J. WARREN, *Int. J. Powder Metall.*, **25** (1989) 337.
9. Y. KIYOTA, J. OHTA, I. SAKURADA, H. OHTSUBO and S. TAKAJO, in "Advances in powder metallurgy", Vol. 3, edited by E. R. Andreotti and P. J. McGeehan (Metal Powder Industries Federation, Princeton, NJ, 1990) p. 455.
10. Y. H. HO and S. T. LIN, *Metall. Mater. Trans. A*, **26A** (1995) 133.
11. C. J. SMITHELLS and E. A. BRANDES, in "Metal reference book", 5th Edn. (Butterworths, London, 1977) p. 935.
12. C. H. SAE, M.S. thesis, National Taiwan University, Taipei, Taiwan, (1995) p. 38.
13. B. D. CULLITY, in "Elements of X-ray diffraction", 2nd Edn. (Addison-Wesley, Reading, MA, 1978) p. 376.
14. S. T. LIN , R. M. GERMAN, K. F. HENS and D. LEE, in "Advances in powder metallurgy", Vol. 3, edited by E. R. Andreotti and P. J. McGeehan (Metal Powder Industries Federation, Princeton, NJ, 1990) p. 423.
15. P. F. STABLEIN and G. C. KUCZYNSKI, *Acta Metall.* **11** (1963) 1327.
16. H. H. HAUSNER, in "Handbook of powder metallurgy" (Chemical Publishing Co., New York, 1973) Tables 9.2 and 9.3.

Received 25 March
and accepted 8 October 1996